Article DOI: https://doi.org/10.3201/eid3108.241137

Emergence of Novel Fluoroquinolone Resistance Mutations in *Mycoplasma bovis*, China, 2008–2023

Appendix

Additional Comments

Traceback analyses using the PubMLST database (https://pubmlst.org; 10 March 2024) revealed that sequence type (ST) 52 had been isolated from cattle in Australia and the United States as early as 2006, persisting throughout the subsequent ≈10-year period (*1*,*2*). A previous molecular epidemiologic study of *M. bovis* in Israel found that 87.5% of *M. bovis* isolates transmitted from Australia to Israel belonged to the ST52 genotype (*2*). Importantly, People's Republic of China and Israel have imported cattle from Australia over the past decade (*2*). Those findings suggest that ST52, which is disseminated widely in People's Republic of China, could share a common Australian origin with similar strains identified in Israel. This complexity underscores the global nature of the cattle trade and its implications for pathogen transmission.

Notably, studies have reported that a mutation from Asp to Asn at position 362 in the GyrB protein of *M. bovis* might increase resistance to fluoroquinolone antibiotics (*3*,*4*). However, we investigated 77 *M. bovis* strains prevalent in People's Republic of China and found that all exhibited the D362N mutation in GyrB (Appendix Figure 2, panel D). Despite this mutation, some isolates displayed extreme sensitivity to fluoroquinolone antibiotics. The *M. bovis* strains from People's Republic of China in our investigation belonged to the clonal complex (CC) 52, but corresponding mutations were not found in isolates from CC12 (Appendix

Figure 1, panel B; Appendix Figure 4). This observation suggests that the Asp→Asn mutation at position 362 in GyrB is not a necessary determinant for fluoroquinolone resistance in *M. bovis*, but may be associated with specific characteristics of certain genotypes.

Additional Methods

Data

Data on *M. bovis* isolates were obtained on 10 March 2024 from the PubMLST database (n = 1,315, comprising 824 characterized and 491 uncharacterized multilocus sequence typing (MLST) genotypes; Appendix Table 2). Then, *M. bovis* genomes from 16 provinces in People's Republic of China from 2008 to 2023 retrieved from GenBank (n = 43) and the whole-genome sequences of *M. bovis* strains from our study (n = 34) were used to explore the genetic evolutionary relationships of *M. bovis* in People's Republic of China (n = 77 in total) (Appendix Table 1).

Phylogenetic Tree

Using the default settings of Snippy v4.6 (https://github.com/tseemann/snippy), comparative genomic analysis was conducted on 77 *M. bovis* genomes against the reference genome (*M. bovis* HB0801) employing BWA-MEM version 0.7.12 to map short reads. Snippy generated a "core complete alignment" file. Single-nucleotide polymorphisms (SNPs) were extracted and recombination sequences were removed by using Gubbins version 2.4.1 (*5*). Then, the SNP alignment file was used to construct a maximum-likelihood phylogenetic tree via FastTree v2.1.3 (www.microbesonline.org/fasttree), which was visualized and annotated subsequently by using tvBOT (*6*).

Sequence Alignment and Visualization

Multiple sequence alignment of the amino acid sequences encoded by the *parC*, *gyrA*, and *gyrB* genes from *M. bovis* isolates was performed by using MAFFT 7.0 software (*7*). Subsequently, the alignment results were visualized by using the ESPript 3.0 server (*8*).

Whole-Genome Sequencing

The above mentioned 38 clinical strains isolated in People's Republic of China (n = 34), Hungary (n = 2), France (n = 1), and the United States (n = 1) and preserved in our laboratory underwent whole-genome sequencing (WGS). PacBio third-generation sequencing was used for 3 strains (08M, 07801, and N44), and Illumina (https://www.illumina.com) second-generation high-throughput sequencing was used for the remaining 35 strains.

Illumina WGS

For Illumina paired-end WGS, ≥3 μg genomic DNA per sample was used to construct sequencing libraries with ≈450-bp insert sizes, according to Illumina's protocol. The genomic DNA was fragmented to the desired size by using Covaris, followed by end repair using T4 DNA polymerase. Adenylation of the blunt ends facilitated adaptor ligation. Fragment selection was achieved through gel electrophoresis and subsequent PCR enrichment and indexing. Library quality was assessed before sequencing on an Illumina NovaSeq 6000 platform (150 bp × 2) by Shanghai Biozeron Biotechnology Co., Ltd (http://www.biozeron.com).

PacBio WGS

For PacBio WGS, PacBio Sequel IIe technology (Pacific Biosciences, https://www.pacb.com) was used; DNA was processed into SMRTbell libraries by using an Express Template Prep Kit 2.0 (Pacific Biosciences) per the manufacturer's instructions. The samples were combined into a single multiplexed library and underwent size selection via Sage Sciences' BluePippin by following the 0.75% Dye-Free (DF) Marker S1 High-Pass 6–10 kb v3 protocol with a cutoff of 8000 bp. Thereafter, the SMRTbell library was prepared for sequencing by annealing and binding according to the SMRT Link Set Up guidelines on the Sequel IIe system.

Genome Assembly

Raw paired-end reads were trimmed and quality controlled using Trimmomatic, producing clean data for further analysis. PacBio reads were converted to FASTQ format via

Samtools. Illumina datasets were employed to assess genome complexity and to correct the PacBio long reads. Genome assembly was conducted with Unicycler v0.4.8 using default settings, yielding optimal assembly outcomes. GC content, depth, and genome size were determined using custom Perl scripts to detect potential contamination. Each assembled strain genome was circularized using Circlator version 1.5.5.

Molecular Dynamic Simulations

Each protein structure (ParC and GyrA) was converted into a pdbqt file using AutoDockTools v4.2.6 within MGLTools software (*9*). Each small-molecule ligand (enrofloxacin, danofloxacin, and ciprofloxacin) was also processed into pdbqt files using AutoDockTools. A docking box was constructed to encompass the entire protein. Each small-molecule ligand was docked with the protein using Autodock Vina, followed by an analysis of the docking results to evaluate their conformations.

Subsequently, each protein and small-molecule ligand from the docking results were separated. The Antechamber tool within AmberTools version 23 (*10*) was used to generate a force field file for the small-molecule ligand, which was then converted into a Gromacs force field file using the ACPYPE software tool (*11*). The small-molecule ligand was modeled using the GAFF force field, whereas the protein was simulated with the AMBER14SB force field and TIP3P water model. Files for the protein and small-molecule ligand were merged to construct a simulation system for the complex. Molecular dynamic (MD) simulations were conducted using the Gromacs2022 program, under constant temperature and pressure conditions with periodic boundary conditions. Throughout the MD simulation, all interactions involving hydrogen bonds were constrained using the LINear Constraint Solver algorithm, with an integration step size of 2 fs. The electrostatic interactions were calculated using the particle-mesh Ewald method with a cutoff of 1.2 nm. Nonbonded interactions had a cutoff of 10 Å, with an update every 10 steps. The V-rescale thermostat method was employed to maintain the simulation temperature at 298 K, while the Berendsen barostat method was used to maintain the pressure at 1 bar. At 298 K, equilibration simulations of both NVT (constant number of particles, volume, and temperature)

and NPT (constant number of particles, pressure, and temperature) were performed for 100 ps, followed by a 100-ns MD simulation of the complex; conformations were saved every 10 ps. Upon completion of the simulation, the trajectory was analyzed, and the MM-PBSA binding free energy of the complex was calculated using the g_mmpbsa program.

MIC Assays

Pleuropneumonia-like organisms (PPLO) broth was supplemented with 2 g/L sodium pyruvate, 2 g/L glucose, 10% yeast extract, and 10% horse serum to create a culture medium (pH 7.6–7.8) for *Mycoplasma* species. For each MIC assay, antibiotic dilutions were prepared fresh according to instructions. There were 2-fold serial dilutions (ranging from 0.0625 to 128 μg/mL) of fluoroquinolones comprising enrofloxacin (catalog number E302224–1g; Solarbio, https://www.solarbio.com), danofloxacin (D132445–100mg; Solarbio), and ciprofloxacin (C304792–25 g; Solarbio). MIC assays were conducted in accordance with the recommendations of Hannan and colleagues (*12*) and Gütgemann and collaborators (*13*) with slight modifications using an inoculation concentration of 10^3 colony forming units/mL for each tested strain. Three replicates of each of the clinical isolates and reference strain (*M. bovis* PG45) were tested in 96-well microtiter plates. In addition, wells in the 96-well microtiter plates were used for growth control (culture medium containing inoculums of *Mycoplasma* species but no antibiotics), sterility control (culture medium containing neither antibiotics nor inoculums of *Mycoplasma* species), and drug control (culture medium containing only the lowest antibiotic dilution).

Data Availability

Publicly available sequence data were downloaded from PubMLST (https://pubmlst.org/organisms/mycoplasma-bovis) and NCBI (https://www.ncbi.nlm.nih.gov/datasets/genome/?taxon=28903).

References

1. Register KB, Lysnyansky I, Jelinski MD, Boatwright WD, Waldner M, Bayles DO, et al. Comparison of two multilocus sequence typing schemes for *Mycoplasma bovis* and revision of the PubMLST reference method. J Clin Microbiol. 2020;58:e00283-20. PubMed https://doi.org/10.1128/JCM.00283-20

2. Yair Y, Borovok I, Mikula I, Falk R, Fox LK, Gophna U, et al. Genomics-based epidemiology of bovine *Mycoplasma bovis* strains in Israel. BMC Genomics. 2020;21:70. PubMed https://doi.org/10.1186/s12864-020-6460-0

3. Khalil D, Becker CAM, Tardy F. Alterations in the quinolone resistance-determining regions and fluoroquinolone resistance in clinical isolates and laboratory-derived mutants of *Mycoplasma bovis*: not all genotypes may be equal. Appl Environ Microbiol. 2015;82:1060–8. PubMed https://doi.org/10.1128/AEM.03280-15

4. Gautier-Bouchardon AV. Antimicrobial resistance in *Mycoplasma* spp. Microbiol Spectr. 2018;6:10.1128/microbiolspec.arba-0030-2018. PubMed https://doi.org/10.1128/microbiolspec.ARBA-0030-2018

5. Croucher NJ, Page AJ, Connor TR, Delaney AJ, Keane JA, Bentley SD, et al. Rapid phylogenetic analysis of large samples of recombinant bacterial whole genome sequences using Gubbins. Nucleic Acids Res. 2015;43:e15. PubMed https://doi.org/10.1093/nar/gku1196

6. Xie J, Chen Y, Cai G, Cai R, Hu Z, Wang H. Tree Visualization By One Table (tvBOT): a web application for visualizing, modifying and annotating phylogenetic trees. Nucleic Acids Res. 2023;51:W587–92. PubMed https://doi.org/10.1093/nar/gkad359

7. Katoh K, Standley DM. MAFFT multiple sequence alignment software version 7: improvements in performance and usability. Mol Biol Evol. 2013;30:772–80. PubMed https://doi.org/10.1093/molbev/mst010

8. Robert X, Gouet P. Deciphering key features in protein structures with the new ENDscript server. Nucleic Acids Res. 2014;42:W320–4. PubMed https://doi.org/10.1093/nar/gku316

9. Arcon JP, Modenutti CP, Avendaño D, Lopez ED, Defelipe LA, Ambrosio FA, et al. AutoDock Bias: improving binding mode prediction and virtual screening using known protein-ligand interactions. Bioinformatics. 2019;35:3836–8. PubMed https://doi.org/10.1093/bioinformatics/btz152

10. Case DA, Aktulga HM, Belfon K, Cerutti DS, Cisneros GA, Cruzeiro VWD, et al. AmberTools. J Chem Inf Model. 2023;63:6183–91. PubMed https://doi.org/10.1021/acs.jcim.3c01153

11. Kagami L, Wilter A, Diaz A, Vranken W. The ACPYPE web server for small-molecule MD topology generation. Bioinformatics. 2023;39:btad350. PubMed https://doi.org/10.1093/bioinformatics/btad350

12. Hannan PC. Guidelines and recommendations for antimicrobial minimum inhibitory concentration (MIC) testing against veterinary *Mycoplasma* species. International Research Programme on Comparative Mycoplasmology. Vet Res. 2000;31:373–95. PubMed https://doi.org/10.1051/vetres:2000100

13. Gütgemann F, Müller A, Churin Y, Kumm F, Braun AS, Yue M, et al. Toward a method for harmonized susceptibility testing of *Mycoplasma bovis* by broth microdilution. J Clin Microbiol. 2023;61:e0190522. PubMed https://doi.org/10.1128/jcm.01905-22

Appendix Table 1. Whole-genome sequencing data for *Mycoplasma bovis* strains from this study and GenBank

Strain	Country	Region	GenBank accession no.*
M. bovis GT01	China	Asia	This study
M. bovis GT02	China	Asia	This study
M. bovis 1523	China	Asia	This study
M. bovis 1527	China	Asia	This study
M. bovis 22762	China	Asia	This study
M. bovis 0709	China	Asia	This study
M. bovis 07801	China	Asia	This study
M. bovis 0794	China	Asia	This study
M. bovis 13690	China	Asia	This study

Strain	Country	Region	GenBank accession no.*
M. bovis 14043	China	Asia	This study
M. bovis 1F	China	Asia	This study
M. bovis 1XS	China	Asia	This study
M. bovis 2206	China	Asia	This study
M. bovis 2213	China	Asia	This study
M. bovis 7118	China	Asia	This study
M. bovis NF22	China	Asia	This study
M. bovis NM-1	China	Asia	This study
M. bovis NM-2	China	Asia	This study
M. bovis NM-3	China	Asia	This study
M. bovis OF2	China	Asia	This study
M. bovis P-1	China	Asia	This study
M. bovis P-2	China	Asia	This study
M. bovis WW-1	China	Asia	This study
M. bovis WW-2	China	Asia	This study
M. bovis WW-4	China	Asia	This study
M. bovis WW-5	China	Asia	This study
M. bovis Z-0093	China	Asia	This study
M. bovis Z-0096	China	Asia	This study
M. bovis Z-123001	China	Asia	This study
M. bovis Z-Y	China	Asia	This study
M. bovis ZY-J3	China	Asia	This study
M. bovis ZY-J4	China	Asia	This study
M. bovis ZY-J5	China	Asia	This study
M. bovis 08M	China	Asia	GCF_002009275.1_ASM200927v1_genomic (our lab)
M. bovis NX114	China	Asia	GCF_032463445.1_ASM3246344v1_genomic
M. bovis Tibet-10	China	Asia	GCF_014854615.1_ASM1485461v1_genomic
M. bovis XBY01	China	Asia	GCF_009650115.1_ASM965011v1_genomic
M. bovis FX	China	Asia	GCF_006659345.1_ASM665934v1_genomic
M. bovis EZ-2	China	Asia	GCF_006659305.1_ASM665930v1_genomic
M. bovis ZMD	China	Asia	GCF_006659275.1_ASM665927v1_genomic
M. bovis KEQ	China	Asia	GCF_006659265.1_ASM665926v1_genomic
M. bovis XM-RG	China	Asia	GCF_006659245.1_ASM665924v1_genomic
M. bovis GA	China	Asia	GCF_006659195.1_ASM665919v1_genomic
M. bovis BZ	China	Asia	GCF_006659175.1_ASM665917v1_genomic
M. bovis SG	China	Asia	GCF_006659165.1_ASM665916v1_genomic
M. bovis XZ-1	China	Asia	GCF_006659155.1_ASM665915v1_genomic
M. bovis SD-130626	China	Asia	GCF_006659145.1_ASM665914v1_genomic
M. bovis YLrengong	China	Asia	GCF_006659125.1_ASM665912v1_genomic
M. bovis YC	China	Asia	GCF_006659075.1_ASM665907v1_genomic

Strain	Country	Region	GenBank accession no.*
M. bovis WX	China	Asia	GCF_006659065.1_ASM665906v1_genomic
M. bovis JX	China	Asia	GCF_006659055.1_ASM665905v1_genomic
M. bovis KLQ	China	Asia	GCF_006659045.1_ASM665904v1_genomic
M. bovis DY	China	Asia	GCF_006659025.1_ASM665902v1_genomic
M. bovis EZ-8	China	Asia	GCF_006658975.1_ASM665897v1_genomic
M. bovis XM	China	Asia	GCF_006658965.1_ASM665896v1_genomic
M. bovis SZ	China	Asia	GCF_006658955.1_ASM665895v1_genomic
M. bovis ZhX	China	Asia	GCF_006658945.1_ASM665894v1_genomic
M. bovis YJ0719	China	Asia	GCF_006658905.1_ASM665890v1_genomic
M. bovis YL0724	China	Asia	GCF_006658885.1_ASM665888v1_genomic
M. bovis NNH	China	Asia	GCF_006658865.1_ASM665886v1_genomic
M. bovis F150tu	China	Asia	GCF_006658855.1_ASM665885v1_genomic
M. bovis JS1075	China	Asia	GCF_006658845.1_ASM665884v1_genomic
M. bovis 1834	China	Asia	GCF_006658825.1_ASM665882v1_genomic
M. bovis TY120615	China	Asia	GCF_006658795.1_ASM665879v1_genomic
M. bovis DYrengong	China	Asia	GCF_006658785.1_ASM665878v1_genomic
M. bovis F150niu	China	Asia	GCF_006658745.1_ASM665874v1_genomic
M. bovis SY	China	Asia	GCF_006658735.1_ASM665873v1_genomic
M. bovis LJ1225	China	Asia	GCF_006658725.1_ASM665872v1_genomic
M. bovis KF	China	Asia	GCF_006658695.1_ASM665869v1_genomic
M. bovis JXXY	China	Asia	GCF_006658685.1_ASM665868v1_genomic
M. bovis YL2086	China	Asia	GCF_006658645.1_ASM665864v1_genomic
M. bovis YL	China	Asia	GCF_006658585.1_ASM665858v1_genomic
M. bovis SZ-0527	China	Asia	GCF_006542475.1_ASM654247v1_genomic
M. bovis EZ-3	China	Asia	GCF_006542465.1_ASM654246v1_genomic
M. bovis XZ-2	China	Asia	GCF_006542455.1_ASM654245v1_genomic
M. bovis 16M	China	Asia	GCF_004792535.1_ASM479253v1_genomic
M. bovis HS-130614	China	Asia	GCF_004751945.1_ASM475194v1_genomic
M. bovis Ningxia-1	China	Asia	GCF_002749575.1_ASM274957v1_genomic
M. bovis NM 2012	China	Asia	GCF_001043135.1_ASM104313v1_genomic
M. bovis CQ-W70	China	Asia	GCF_000696015.1_ASM69601v1_genomic
M. bovis HB0801	China	Asia	GCF_000270525.1_ASM27052v1_genomic
M. bovis Hubei-1	China	Asia	GCF_000219375.1_ASM21937v1_genomic
M. bovis 970139	France	Europe	In this study
M. bovis N43	Hungary	Europe	In this study
M. bovis N44	Hungary	Europe	In this study
M. bovis Madison	USA	North America	In this study
M. bovis PG45	USA	North America	GCF_000183385.1_ASM18338v1_genomic

*Sequences from this study were deposited in the NCBI BioProject database (https://www.ncbi.nlm.nih.gov/bioproject; accession nos. PRJNA1124599–601).

Appendix Table 2. *Mycoplasma bovis* isolates from the PubMLST global database*

Isolate name	Host	Site	Country	Continent	Year	ST
HB0801	bovid	lung	China	Asia	2008	52
63307	bovid	lung	Australia	Oceania	2010	52
86812	bovid	milk	Israel	Asia	2010	52
HAZ1734	bovid	nasal cavity	Japan	Asia	2014	52
NM2012	bovid	joint	China	Asia	2012	52
08M	bovid	lung	China	Asia	2008	52
MJ24	bovid	lung	Canada	North America	2015	52
MJ30	bovid	lung	Canada	North America	2007	52
MJ63	bovid	lung	Canada	North America	2008	52
MJ64	bovid	joint	Canada	North America	2007	52
MJ94	bovid	ear	Canada	North America	2015	52
MJ246	bovid	joint	Canada	North America	2016	52
6099	bovid	milk	Israel	Asia	2007	52
347	bovid	milk	Israel	Asia	2008	52
432	bovid	milk	Israel	Asia	2008	52
928	bovid	milk	Israel	Asia	2008	52
758	bovid	milk	Israel	Asia	2008	52
2621	bovid	milk	Israel	Asia	2008	52
2622	bovid	milk	Israel	Asia	2008	52
5428	bovid	milk	Israel	Asia	2008	52
2715	bovid	milk	Israel	Asia	2008	52
110	bovid	milk	Israel	Asia	2008	52
1662	bovid	milk	Israel	Asia	2008	52
991–2	bovid	milk	Israel	Asia	2008	52
889	bovid	milk	Israel	Asia	2008	52
10–155	bovid	milk	Israel	Asia	2008	52
783	bovid	milk	Israel	Asia	2009	52
26443	bovid	milk	Israel	Asia	2009	52
701	bovid	milk	Israel	Asia	2009	52
299	bovid	milk	Israel	Asia	2010	52
883	bovid	milk	Israel	Asia	2010	52
65714	bovid	milk	Israel	Asia	2011	52
111449	bovid	milk	Israel	Asia	2011	52
108432	bovid	milk	Israel	Asia	2011	52
127377	bovid	milk	Israel	Asia	2012	52
126814	bovid	milk	Israel	Asia	2012	52
129771	bovid	milk	Israel	Asia	2012	52
147529	bovid	milk	Israel	Asia	2012	52
139667	bovid	milk	Israel	Asia	2013	52

Isolate name	Host	Site	Country	Continent	Year	ST
170217	bovid	milk	Israel	Asia	2013	52
170228	bovid	milk	Israel	Asia	2013	52
178843	bovid	milk	Israel	Asia	2013	52
XBY01	bovid	lung	China	Asia	2019	52
209716	bovid	milk	Israel	Asia	2014	52
220642	bovid	milk	Israel	Asia	2015	52
222991	bovid	milk	Israel	Asia	2015	52
227457	bovid	milk	Israel	Asia	2015	52
227456	bovid	milk	Israel	Asia	2015	52
227455	bovid	milk	Israel	Asia	2015	52
227465	bovid	milk	Israel	Asia	2015	52
228404	bovid	milk	Israel	Asia	2015	52
254410	bovid	milk	Israel	Asia	2016	52
280413	bovid	milk	Israel	Asia	2016	52
290360	bovid	milk	Israel	Asia	2017	52
161801	bovid	milk	Russia	Asia	2013	52
2A	bovid	pharynx	Australia	Oceania	2006	52
H	bovid	joint	Australia	Oceania	2006	52
2D	bovid	pharynx	Australia	Oceania	2006	52
1254	bovid	lung	Australia	Oceania	2006	52
261552	bovid	lung	Australia	Oceania	2016	52
41569	bovid	lung	Australia	Oceania	2009	52
2583	bovid	larynx	Australia	Oceania	2009	52
261553–9503	bovid	joint	Australia	Oceania	2016	52
261553–9655	bovid	joint	Australia	Oceania	2016	52
261552–3688	bovid	lung	Australia	Oceania	2016	52
261552–2741	bovid	lung	Australia	Oceania	2016	52
3893	bovid	lung	Hungary	Europe	2007	52
5180	bovid	lung	Israel	Asia	2006	52
5028	bovid	lung	Israel	Asia	2008	52
18525	bovid	lung	Israel	Asia	2008	52
70262–1	bovid	vulva	Israel	Asia	2010	52
72211	bovid	vulva	Israel	Asia	2010	52
219363	bovid	lung	Israel	Asia	2015	52
268681	bovid	eye	Israel	Asia	2016	52
270940	bovid	lung	Israel	Asia	2016	52
287942	bovid	lung	Israel	Asia	2017	52
236–22	bovid	milk	USA	North America	2008	52
236–27	bovid	milk	USA	North America	2008	52
236–28	bovid	milk	USA	North America	2008	52

Isolate name	Host	Site	Country	Continent	Year	ST
236–48	bovid	milk	USA	North America	2007	52
237–4	bovid	milk	USA	North America	2006	52
JS1075-NHD0955	bovid	lung	China	Asia	2008	52
SZ-NHD0960	bovid	lung	China	Asia	2008	52
1834-NHD0953	bovid	lung	China	Asia	2008	52
EZ-3-NHD0947	bovid	lung	China	Asia	2008	52
XZ-1-NHD0981	bovid	lung	China	Asia	2008	52
XZ-2-NHD0946	bovid	lung	China	Asia	2008	52
FX-NHD0970	bovid	lung	China	Asia	2008	52
NNH-NHD0956	bovid	larynx	China	Asia	2010	52
ZhX	bovid	lung	China	Asia	2010	52
DY-NHD0963	bovid	lung	China	Asia	2010	52
TY-120615-NHD0952	bovid	lung	China	Asia	2012	52
JX-NHD0966	bovid	lung	China	Asia	2012	52
F150tu-NHD0954	bovid	lung	China	Asia	2012	52
F150niu-NHD0949	bovid	lung	China	Asia	2012	52
Dyrengong-NHD0951	bovid	lung	China	Asia	2012	52
HB0801-rengong NHD0989	bovid	lung	China	Asia	2012	52
SY-NHD0950	bovid	lung	China	Asia	2013	52
WX-NHD0964	bovid	joint	China	Asia	2013	52
YC-NHD0967	bovid	milk	China	Asia	2013	52
BZ-NHD0982	bovid	lung	China	Asia	2008	52
XM	bovid	lung	China	Asia	2009	52
XMrengong-NHD0985	bovid	lung	China	Asia	2012	52
LJ1225-NHD0945	bovid	lung	China	Asia	2009	52
YL-NHD0941	bovid	lung	China	Asia	2009	52
KF	bovid	lung	China	Asia	2009	52
YL0724-NHD0957	bovid	lung	China	Asia	2009	52
YJ0719-NHD0958	bovid	lung	China	Asia	2012	52
KEQ-NHD0988	bovid	lung	China	Asia	2010	52
KLQ	bovid	lung	China	Asia	2010	52
ZMD	bovid	lung	China	Asia	2011	52
YLrengong-NHD0968	bovid	lung	China	Asia	2012	52
YL2086	bovid	lung	China	Asia	2012	52
JXXY	bovid	lung	China	Asia	2012	52
GA-NHD0984	bovid	lung	China	Asia	2012	52
SG-NHD0983	bovid	lung	China	Asia	2013	52
SD-130626-NHD0969	bovid	lung	China	Asia	2013	52
16M	bovid	lung	China	Asia	2016	52
HS-130614	bovid	unknown	China	Asia	2013	52

Isolate name	Host	Site	Country	Continent	Year	ST
JZBTM	bovid	milk	China	Asia	2019	52
HBXTBTM	bovid	milk	China	Asia	2019	52
SD1901	bovid	milk	China	Asia	2019	52
MJ255	bovid	lung	Canada	North America	2017	52
MJ256	bovid	joint	Canada	North America	2017	52
MJ257	bovid	lung	Canada	North America	2017	52
MJ270	bovid	joint	Canada	North America	2017	52
MJ279	bovid	lung	Canada	North America	2017	52
MPLM0631	bovid	joint	Canada	North America	2007	52
MB651	calf	lung	Turkey	Asia	2021	52
Hubei-1	bovid	lung	China	Asia	2008	53
Ningxia-1	bovid	lung	China	Asia	2013	54
EZ-2	bovid	unknown	China	Asia	2008	56
CQ-W70	bovid	lung	China	Asia	2009	72
EZ-8-NHD0962	bovid	lung	China	Asia	2008	72
SZ-0527	bovid	unknown	China	Asia	2012	87
NMH7	bovid	milk	China	Asia	2018	89
NMH10	bovid	milk	China	Asia	2018	89
HBCB01	bovid	lung	China	Asia	2019	89
ShaanxiBTM01	bovid	milk	China	Asia	2018	90
HBBDBTM	bovid	milk	China	Asia	2018	90
HBLFBTM01	bovid	milk	China	Asia	2018	90

*PubMLST database (https://pubmlst.org). ST, sequence type.

Appendix Table 3. Calculation of the binding free energies of wild-type and mutant *Mycoplasma bovis* GyrA and ParC proteins with ciprofloxacin*

	Binding energy, KJ/mol (SD)						
Complex†	ΔE_{vdw}	ΔE_{ele}	ΔE_{pol}	ΔE_{nonpol}	ΔE_{MMPBSA}‡	$-T\Delta S$	ΔG_{bind}§
GyrA							
Wild type	–176.75	–49.182	179.361	–22.275	–68.845	22.730 (2.408)	–46.115 (8.72)
	(6.949)	13.173)	(19.121)	(0.057)	(6.711)		
S150F	–116.887	–7.279 (2.208)	77.115 (3.760)	–16.375	–63.426	19.997 (0.599)	–43.429
	(1.918)			(0.276)	(0.139)		(0.500)
S150Y	–128.426	–28.583	136.495	–17.798	–38.313	28.071 (3.504)	–10.242
	(2.159)	(1.907)	(6.246)	(0.248)	(5.766)		(2.892)
ParC							
Wild type	–124.659	–22.821	102.890	–16.802	–61.392	41.418 (3.982)	–19.973
	(4.152)	(7.459)	(13.640)	(0.471)	(4.670)		(2.445)
S91R	–114.985	–61.062	179.926	–17.683	–13.804	40.665 (4.608)	26.861 (5.140)
	(5.927)	(4.335)	(9.898)	(0.723)	(0.563)		

*ΔE_{ele}, electrostatic energy; ΔE_{MMPBSA}, binding energy; ΔE_{nonpol}, nonpolar solvation energy; ΔE_{pol}, polar solvation energy; ΔE_{vdw}, van der Walls energy; $-T\Delta S$, entropic contribution.

†*Escherichia coli* K12 strain GyrA mutation S150F corresponds to the S83F mutation and *E.coli* S150Y corresponds to the S83Y mutation in GyrA of *M. bovis* isolates. *Escherichia coli* K12 strain S91R mutation in ParC corresponds to the S80R mutation site in ParC of *M. bovis* isolates.

‡$\Delta E_{MMPBSA} = \Delta E_{ele} + \Delta E_{vdw} + \Delta E_{pol} + \Delta E_{nonpol.}$

§$\Delta G_{bind} = \Delta E_{MMPBSA} - T\Delta S$.

Appendix Table 4. Molecular characterization of GyrA and ParC in *Mycoplasma bovis* isolates that had different susceptibility to enrofloxacin, danofloxacin, and ciprofloxacin*

		Amino acid mutations in QRDRs		Fluoroquinolone MICs, μg/mL		
M. bovis isolates	ST	GyrA	ParC	Enrofloxacin	Danofloxacin	Ciprofloxacin
PG45†‡	12	S83	S80, D84	0.125	0.125	0.25
Madison‡	12	S83	S80, D84	0.125	0.125	0.25
Z-0093‡	New	S83	S80, D84	0.125	0.125	0.25
ZY‡	New	S83	S80, D84	0.125	0.125	0.25
GT01‡	52	S83	S80, D84	0.125	0.125	0.25
WW-1‡	52	S83	S80, D84	0.125	0.125	0.25
OF2‡	52	S83	S80, D84	0.125	0.125	0.25
ZY-J4	52	S83F	S80, D84G	4	2	4
ZY-J5	52	S83F	S80, D84G	4	2	4
ZY-J3	52	S83F	S80R, D84	8	4	8
P-1	52	S83F	S80R, D84	8	4	16
P-2	52	S83F	S80R, D84	8	4	16
NM-1	52	S83Y	S80R, D84	8	4	16

		Amino acid mutations in QRDRs		Fluoroquinolone MICs, μg/mL		
M. bovis isolates	ST	GyrA	ParC	Enrofloxacin	Danofloxacin	Ciprofloxacin
NM-2	52	S83Y	S80R, D84	8	4	16
NM-3	52	S83Y	S80R, D84	8	4	16

*QRDR, quinolone resistance-determining regions; ST, sequence type.

†Standard strain of *Mycoplasma bovis*.

‡Clinical isolate with no amino acid mutations in the GyrA or ParC proteins.

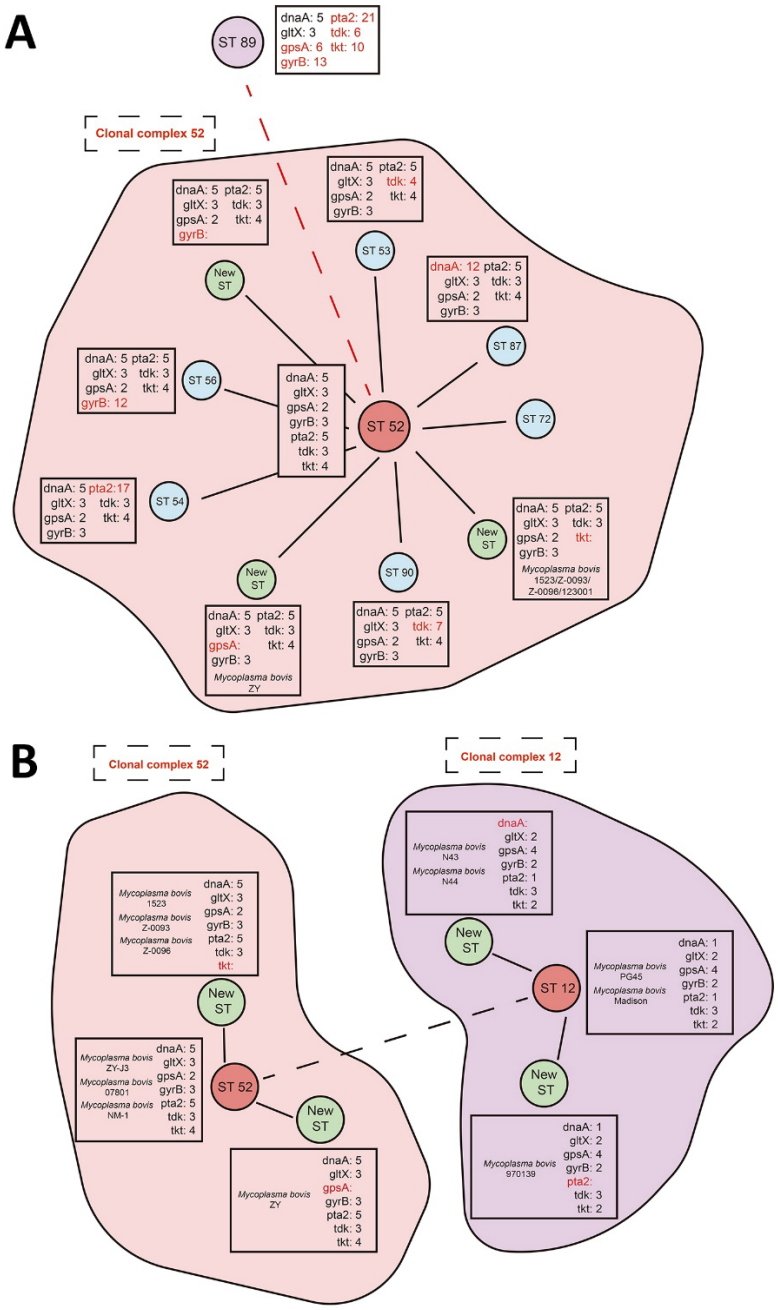

Appendix Figure 1. Multilocus sequence typing genotypes of prevalent *M. bovis* isolates in China. A) Clonal complex (CC) 52 is formed with ST52 (red) as the core genotype. Blue indicates other ST genotypes belonging to CC52. Green indicates new ST genotypes belonging to CC52. Purple indicates strains that do not belong to CC52. B) Analysis of *M. bovis* isolates from CC52 and CC12. *M. bovis* strains 1523, Z-0093, Z-0096, and ZY belong to the CC52 with ST52 as the core genotype. *M. bovis* strains N43, N44, and 970139 belong to the CC12 with ST12 as the core genotype. ST, sequence type.

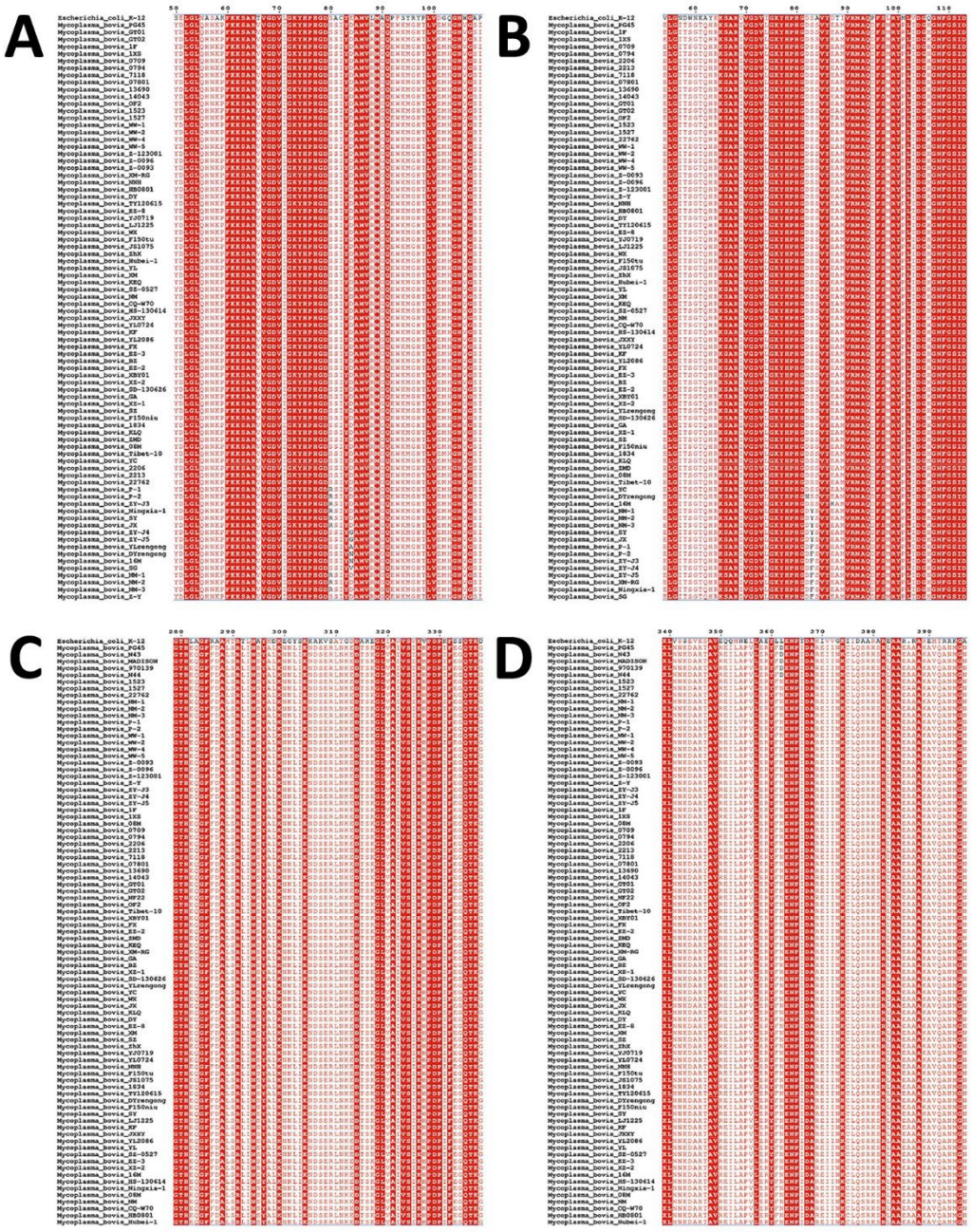

Appendix Figure 2. Amino acid sequence alignments of proteins from *Mycoplasma bovis* isolates from China. A, B) Multiple alignments of ParC (A) and GyrA (B) amino acid sequences indicating mutations. C, D) Sequence alignments of key quinolone resistance determining regions within GyrB. Regions surrounding the GyrB Val320 residue (C) and Asp362 residue (D).

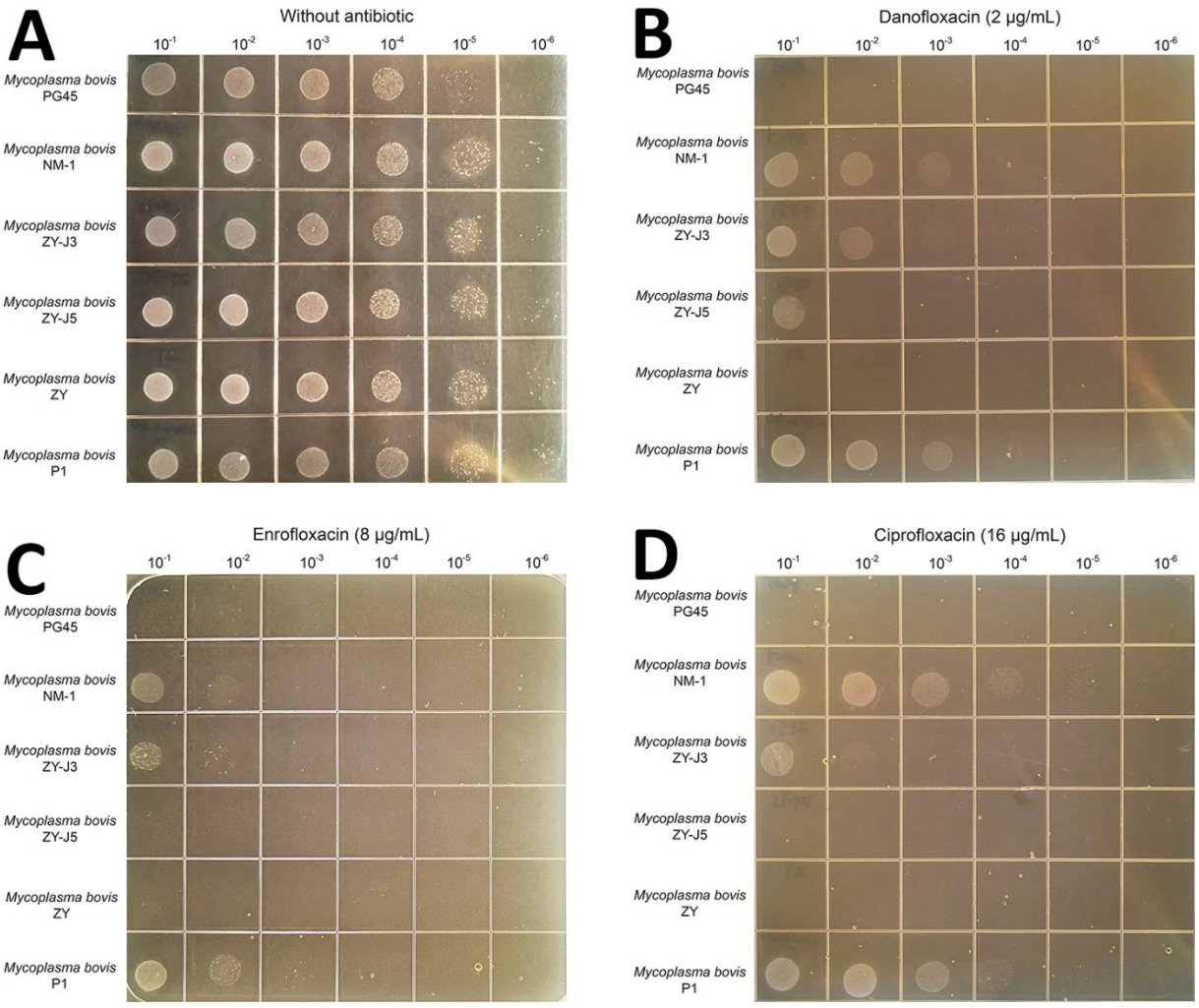

Appendix Figure 3. Drug susceptibility spot-plate assay of *Mycoplasma bovis* ParC and GyrA mutant strains. A–D) Spot-plate assay of *M. bovis* isolates on agar medium containing no antibiotic (A), danofloxacin (B), enrofloxacin (C), and ciprofloxacin (D). *M. bovis* nonmutant strains PG45 and ZY were used as controls.

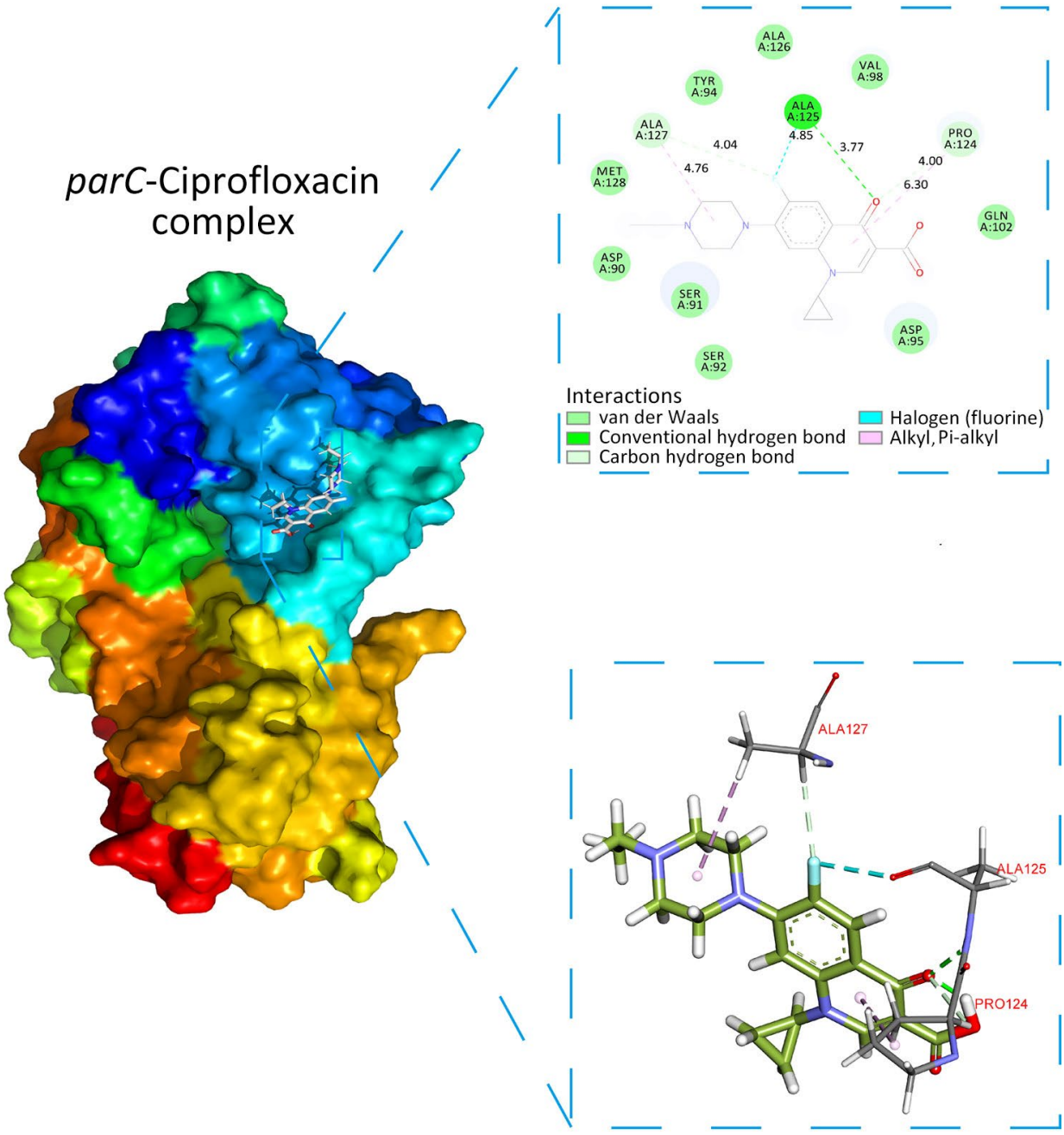

Appendix Figure 4. Molecular dynamic simulation of wild-type *Mycoplasma bovis* ParC protein bound to ciprofloxacin. ALA125 in ParC protein forms a hydrogen bond with the small-molecule ligand ciprofloxacin, whereas ALA127 and PRO124 form Pi-alkyl and alkyl hydrophobic interactions, and residues, such as SER91, TYR94, and VAL98, form van der Waals interactions with the small-molecule ligand. Zoomed areas show specific amino acid interactions with the drug.